Unsupervised Decoding of Multi-Finger Forces Using Neuronal Discharge Information with Muscle Co-Activations

Long Meng
Department of Mechanical Engineering
Pennsylvania State University
University Park, PA, USA
lmm7405@psu.edu

Xiaogang Hu
Department of Mechanical Engineering
Pennsylvania State University
University Park, PA, USA
xxh120@psu.edu

2024 IEEE 4th International Conference on Human-Machine Systems (ICHMS) | 979-8-3503-1579-0/24/$31.00 ©2024 IEEE | DOI: 10.1109/ICHMS59971.2024.10555639

***Abstract*—Accurate finger force prediction is essential for intuitive human-machine interactions. Various studies have attempted to develop reliable decoders for multi-finger force prediction for the control of assistive robotic hands. However, most approaches were implemented in a supervised manner, i.e., data labels (e.g., finger forces) were needed to train or refine models, which might not be appropriate in certain situations, particularly in the cases of individuals with an arm amputation. In addition, previous studies have not addressed interference from the co-activations of unintended finger muscles. However, finger co-activations occur naturally in daily activities. Therefore, we developed an unsupervised neural-drive approach for simultaneous and continuous multi-finger force predictions, considering finger muscle co-activations instead of avoiding them. To this end, we collected high-density surface electromyogram (sEMG) signals from the forearm extensor muscle during single- and multi-finger isometric contraction tasks. Motor units (MUs) were extracted from sEMG signals of the single-finger tasks. Considering the different contribution of each MU, we assigned weights to MUs based on the firing statistics of the MUs for the target finger across trials. Due to the co-activation effect, where MUs from other fingers may influence the force of the target finger, we introduced an MU sharing procedure to incorporate these MUs. Compared with the supervised sEMG-amplitude methods, our approach demonstrated superior force prediction performance, as evidenced by a higher R^2 (0.72±0.11 vs. 0.64±0.073) and a lower root mean square error (5.95±1.43 %MVC vs. 7.47±1.81 %MVC). Our approach has the potential to enable intuitive neural-machine interfaces, allowing a wide range of human-machine system applications.**

Keywords—unsupervised neural decoding, finger force prediction, finger co-activations, biosignal processing

I. Introduction

Finger force prediction plays an important role in human-machine systems, including advanced prosthetic control, virtual reality, and remote surgical operations [1]. To maximize the wide use of those applications, it is essential to accurately predict finger forces for the natural and intuitive interactions between humans and machines. Finger force prediction based on surface electromyogram (sEMG) signals has gained increasing attention due to its noninvasive nature and its capacity to predict both isometric and isotonic finger forces in both extension and flexion directions [2], [3].

sEMG signals are formed by the summation of motor unit action potentials (MUAPs) [4]. Previous studies [5], [6] have applied models for continuous finger force prediction based on the variation of macroscopic features (directly extracted from global sEMG signals, such as sEMG amplitude). Intuitively, by placing electrodes on target muscle areas, it is possible to capture the muscle activity related to the finger movements. The captured information can then be translated into input for machine control. However, the anatomical proximity of individual finger muscle compartments poses a challenge. An electrode channel may capture activities from adjacent muscle compartments associated with different fingers. These interferences greatly challenge the accurate prediction of finger forces using macroscopic features.

With the development of wearable techniques, particularly in the context of flexible high-density surface electromyography (sEMG) electrode arrays, it is possible to conduct sEMG-related analysis at the microscopic level (via decomposed neuronal discharge events) [7], not just limited to using macroscopic features. Previous studies [5], [6], [8], [9] have revealed the effectiveness of finger force prediction using the neural drive, represented by the populational discharge frequency of motor unit (MUs). Neural-drive approaches can effectively address the potential interferences encountered in macroscopic feature-based methods. However, these studies utilized supervised approaches, necessitating measured forces for model training and refinement procedures, which are not suitable for individuals who have lost hand functionality. In addition, most studies [8] made efforts to isolate co-activations from unintended fingers for an enhanced finger force prediction. However, given that co-activations are both inevitable and commonplace, incorporating them into force prediction is more natural than attempting to isolate them.

To address these challenges, we conducted the neural-drive-based multi-finger force prediction in an unsupervised manner. Considering that MU contributions vary for the target finger, we implemented a weighting strategy. This strategy assigns weights to each MU based on its firing frequency for the target finger across trials. Due to the co-activation effect, the movement of other fingers may also contribute to the force of the target finger. We employed an MU sharing procedure, by incorporating MUs from other fingers, to facilitate more accurate and nature human-machine interaction. To be specific, subjects were required to perform single-finger tasks (for MU extraction) and multi-finger tasks (for MU weight assignment, MU sharing procedure, and model performance evaluation). Our model demonstrated superior force prediction performance compared to supervised sEMG-amplitude-based models. This holds promise for more accurate human-machine interactions across a broader range of applications.

This study was supported in part by the National Science Foundation (CBET-2246162, IIS-2330862, IIS-2319139) and the Department of Defense (W81XWH2110185).

II. METHODS

A. Data Acquisition and Preprocessing

We recruited 8 participants (1 female and 7 males, aged 21 to 35 years) without known neuromuscular disorders. They signed the informed consent for the protocols approved by the Institutional Review Board of the Pennsylvania State University.

Before data collection, we allowed subjects to adjust their chair height for comfort. The wrist was held in a neutral position, and the four involved fingers (index, middle, ring, and little) were secured to four load cells (SM-200N, Interface). Finger forces were recorded at a sampling frequency of 1000 Hz and were displayed in real time to better track designed target force trajectories, as shown in Fig. 1. To record sEMG, we covered the extensor digitorum communis (EDC) muscle with an 8 × 20-electrode array (electrode diameter: 3 mm, inter-electrode distance: 10 mm). The monopolar sEMG signals were sampled at 2048 Hz using the EMG-USB2+ (OT Bioelettronica, Torino, Italy), with a gain of 1000, and a pass band of 10–900 Hz.

A large enslaving effect between the ring and little fingers has been revealed by previous studies. Based on the observation of sEMG signals, the activation patterns of EDC muscle compartments related to the ring and little fingers were also similar. Therefore, we required subjects to concurrently extend the ring and little fingers. The measured forces of the two fingers were summed up as the ring-little finger force.

We first obtained the maximum voluntary contraction (MVC) forces of each finger by asking subjects to separately perform the maximum isometric extension of individual fingers. Subsequently, subjects performed both single-finger and multi-finger isometric extension tasks. In each single-finger trial (see Fig. 1(a)), subjects followed a 21-second trapezoid force trajectory with a target finger (the ring and little fingers were considered as one finger due to the enslaving effect). A total of 15 single-finger trials (3 fingers × 5 trials/finger) were recorded. For multi-finger tasks, subjects used at least two fingers, as illustrated in Fig. 1(b) and 1(c). The three-finger tasks lasted 18 seconds, and the two-finger tasks lasted 12 seconds. Correspondingly, a total of 32 trials were performed. Co-contractions of unintended fingers were allowed for the multi-finger tasks, getting close to practical scenarios.

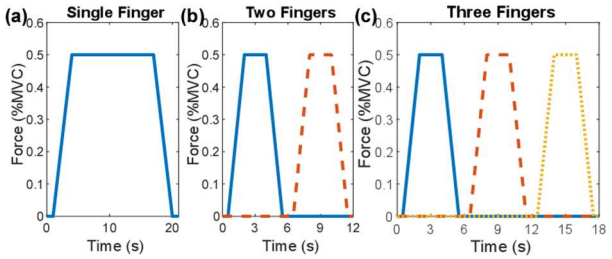

Fig. 1. Force trajectories. Each color denotes one finger.

B. Unsupervised Neural-Drive Approach

As shown in Fig. 2, the unsupervised neural-drive approach mainly included: 1) Initial MU extraction. We extracted MUs from single-finger trials, and MUs extracted from same-finger trials were pooled together, termed raw MUs. 2) MU weight assignment and sharing. To prevent in-sample optimization bias, we adopted a two-fold validation protocol to divide 3-finger trials into two sets. One set was used as the refinement dataset. The other set and all two-finger trials were used as the testing dataset. In the refinement phase, we assigned weights to MUs, including those contributing to the target finger's force from other fingers, termed shared MUs. 3) Force prediction. The force prediction was performed using shared MUs and their corresponding weights.

- MU Extraction

The fast independent component analysis (FastICA) algorithm [10], known for its high decomposition efficiency, is widely used in sEMG decomposition. Therefore, we extracted MUs from single-finger tasks using the FastICA algorithm. To be specific, we calculated mean root mean square (RMS) values of 160-channel sEMG signals using single tasks of the same finger. For each finger, we selected 60 channels that exhibited the highest RMS values. Then, we obtained the union of the three sets for the following analyses. Signals of selected channels were duplicated by a factor of 10 and were further whitened for the FastICA-based decomposition with up to 200 iteration procedures. The decomposed MUs with a low silhouette measure (SIL$<$0.5) were excluded. Lastly, MUs from the same-finger tasks were pooled together. Accordingly, we obtained the separation matrixes, $\boldsymbol{B}_{1,\mathrm{I}}$, $\boldsymbol{B}_{1,\mathrm{M}}$ and $\boldsymbol{B}_{1,\mathrm{RL}}$, where I, M and RL represent index, middle and ring-little fingers, respectively.

- MU Weight Assignment and Sharing

Co-activations of unintended fingers are inevitable, even when we attempt to isolate the force of intended fingers. Instead of attempting to eliminate the co-activations in algorithms, it is more natural to control the human-machine systems by incorporating an MU weighting and sharing strategy. This approach can accommodate and harness these involuntary movements for enhanced precision and control.

A two-fold validation protocol was used to divide 3-finger trials into two sets. Each set, in turn, served as the refinement data. The other set, along with all 2-finger trials, formed the testing dataset. Due to the co-activations, some MUs were activated for more than one finger. Weights were assigned to each MU based on its contribution to different fingers. Specifically, the following steps were conducted.

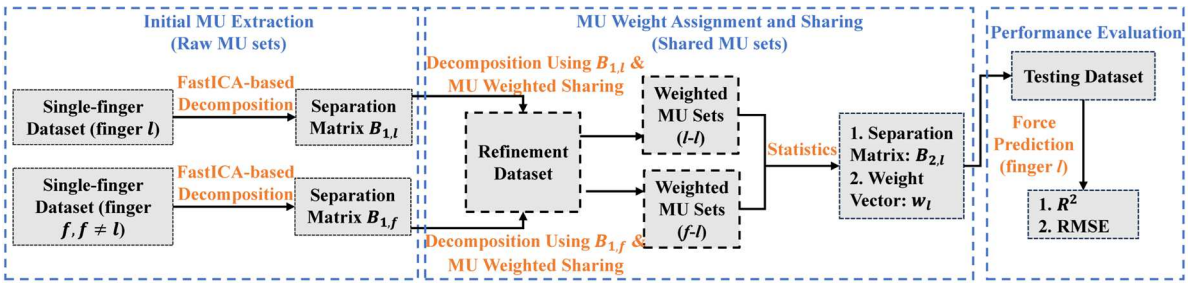

Fig. 2. Framework of the unsupervised neural-drive approach. $f, l \in \{\mathrm{I}, \mathrm{M}, \mathrm{RL}\}$.

1) sEMG decomposition. Given that the computational efficiency of sEMG decomposition via the FastICA algorithm does not suffice for real-time daily use, we directly employed the separation matrix $\boldsymbol{B_{1,l}}$ ($l \in$ {I, M, RL}) to decompose the refinement dataset. After the decomposition, low-quality MUs (SIL<0.5) were removed.

2) Weight assignment. The rationale for the weight assignment is that if one MU is dominant for a finger, the average firing rate during the plateau period of the finger is expected to be greater than that during plateau periods of other fingers. The plateau time periods of the three-finger trials in Fig. 1(c) were 2s-4s, 8s-10s, 14s-16s for the three fingers, respectively. After sEMG decomposition using the separation matrix $\boldsymbol{B}_{1,l}$of the target finger l, we calculated weights of the MUs to the target finger l based on the proportion of dominances for this finger over trials.

3) MU sharing. MUs extracted using separation matrixes of other fingers may contribute to the force of target finger due to the co-activation effect. Those MUs were weighted based on their proportion of dominances over trials for the target finger. All MUs and weights for the target finger were pooled together, termed shared MUs. The corresponding separation matrixes and weight vectors were $\boldsymbol{B}_{2,l}$ and w_l, respectively.

- Force Prediction

Similar to the previous study [8], we built three individual linear models for the force prediction of each of the three fingers. It is worth noting that the measured forces were only used for the force prediction without participating in the MU extraction, weighting and sharing procedures. The linearity of neural-drive signals with finger force allows users to intuitively adjust the force prediction models based on their own sense of the force level they're applying with their fingers. Therefore, the force prediction model can be easily built without measured force in practical use.

For the finger l, we computed high-quality source signals (SIL $>$ 0.6) using $\boldsymbol{B}_{2,l}$. After the duplicated source signal removal procedure, the time courses of firing rate (calculated by a fixed-window strategy with 0.5s window size and 0.1s moving step) and weight vector were updated as $\boldsymbol{F_l} = [\boldsymbol{f}_{1,l}, \cdots, \boldsymbol{f}_{i,l}, \cdots \boldsymbol{f}_{n_l,l}]$ and $\boldsymbol{w_l} = [w_{1,l}, \cdots, w_{i,l}, \cdots w_{n_l,l}]$, where n_l denotes the number of retained MUs for the force prediction of finger l, $\boldsymbol{f}_{i,l}$ and $w_{i,l}$ represent the time course of firing rate and the weight for the ith MU. Correspondingly, the neural-drive signals $\boldsymbol{D_l} = \sum_i \boldsymbol{f}_{i,l} \cdot w_{i,l}$. The neural-drive signals were then smoothed by a Kalman filter and was mapped for force prediction using a linear regression model, depicted as $Force_l = a_l \boldsymbol{D}_l + b_l$, where $Force_l$ denotes the prediction force of finger l, a_l and b_l denote slope coefficient and intercept of the linear regression model, respectively.

Two prevailing indexes, R^2 and the root mean square error (RMSE) between the measured force and predicted force, were employed for prediction performance evaluation.

C. Alternative Approaches for Comparison

The sEMG amplitude has been a prevalent feature for finger force prediction [11]. Two supervised approaches based on sEMG amplitude were explored for comparison.

In the first method, termed the sEMG60-Amp method, we selected 60 channels with top average amplitudes (RMS) for each finger using corresponding single-finger tasks. The testing dataset included all two-finger and three-finger trials. For each trial in the testing dataset, we calculated sEMG amplitude of each channel using the same fixed window sliding strategy. Subsequently, we averaged the sEMG amplitudes of the selected 60 channels, generating a time course of overall amplitude for the target finger, denoted as $\mathbf{A_{60,l}}, l \in \{\mathrm{I}, \mathrm{M}, \mathrm{RL}\}$. Lastly, the $\mathbf{A_{60,l}}$ was used to build a linear regression for force prediction after the Kalman filtering.

In the second approach, we introduced a channel refinement strategy to reduce the sEMG amplitude bias. This approach was termed sEMG-Amp method. The cross-validation strategy, which involves constructing the refinement and testing datasets, was kept consistent with the unsupervised neural-drive approach to ensure a fair comparison. In the channel pool of a given finger, we calculated the R^2 value between the time course of that channel's amplitude and the measured forces of the three fingers across refinement trials. If the R^2 value of one channel with the target finger force was higher than that with forces of other fingers, the channel was retained for the final force prediction. Lastly, we conducted the force prediction using the refined channel pool rather than the 60 channel pool.

D. Statistical Analysis

If the groups being compared satisfied the requirements for parametric analysis, we adopted the Repeated Measures Analysis of Variance (RM ANOVA) and the paired t-test for statistical analysis. If not, we employed the Friedman test and Wilcoxon signed-rank test for the statistical analysis. Holm-Bonferroni correction was applied when necessary to avoid multiple comparison errors. We only reported the corrected p values, with the significance level set at 0.05.

III. Results and Discussion

A. Overall Force Prediction Performance

We compared the finger force predictions across the unsupervised neural-drive, sEMG-Amp, and sEMG60-Amp approaches. As shown in Fig. 3(a), the overall average R^2 values were 0.72±0.11 (Neural-Drive), 0.64±0.073 (sEMG-Amp), and 0.50±0.10 (sEMG60-Amp). A significant difference in R^2 values among the three approaches was revealed by the Friedman test ($\chi^2(2) = 13$, p=0.0015). Further post-hoc analysis using the Wilcoxon signed-rank test showed that the overall R^2 value achieved using the neural-drive approach was significantly higher than that obtained using either sEMG-Amp (p=0.039) or sEMG60-Amp (p=0.012). In addition, the sEMG-Amp approach was significantly better than the sEMG60-Amp method in R^2 value (p=0.012).

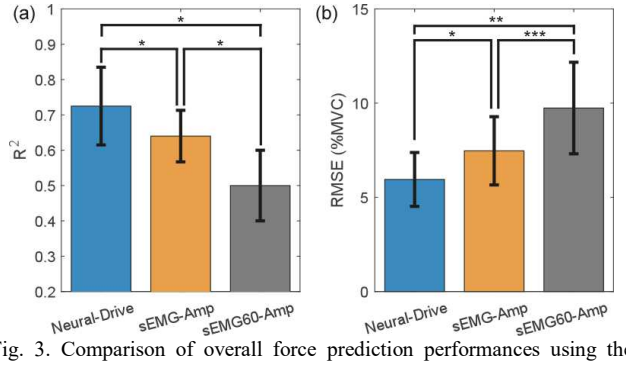

Fig. 3. Comparison of overall force prediction performances using the unsupervised neural-drive, sEMG-Amp, and sEMG60-Amp approaches. * denotes 0.01<p<0.05, ** denotes 0.001<p<0.01, *** denotes p<0.001.

The overall average RMSE values (Fig. 3(b)) were 5.95±1.43 %MVC (Neural-Drive), 7.47±1.81 %MVC (sEMG-Amp), and 9.74±2.43 %MVC (sEMG60-Amp). The one-way RM ANOVA demonstrated that the RMSE values obtained using three approaches were significantly different ($F(2,14)$ =12.49, $p<0.001$). Further paired t-test showed that the RMSE value achieved using the neural-drive approach was significantly lower than that obtained using either sEMG-Amp ($t(7)$=-2.01, p= 0.042) or sEMG60-Amp ($t(7)$=-3.68, p=0.0078). Compared with the sEMG60-Amp method, the sEMG-Amp approach achieved a significantly lower RMSE value ($t(7)$=-7.10, $p<0.001$).

From the results in Fig. 3, we can infer that the channel-refinement procedure was effective in removing channels with large cross-talk of different fingers, resulting in an improvement in the force prediction performance. The force prediction performance can be further improved using the developed unsupervised neural-drive approach, which may fall into the following explanations: 1) Compared to sEMG amplitudes, decomposed binary firing events were less impacted by various interferences, including motion artifacts, signal amplitude cancellation from MU action potential waveform superimposition, background noise, etc. 2) Despite conducting a channel-refinement procedure for the sEMG-Amp method, some channels might still receive cross-talk from other fingers due to the proximity of finger muscle compartments, resulting in inaccurate force estimations. 3) Rather than attempting to eliminate co-activations from other fingers, we acknowledged their inevitable contribution to the target force, which led to more practical force predictions.

B. Finger-Specific force prediction performance

Fig. 4 presents the force prediction performances of the three approaches on each finger. As shown in Fig. 4(a), a significant overall difference in R^2 values was found for the index finger (One-way RM ANOVA: $F(2,14)$ =25.14, $p<0.001$) and the ring-little finger (Friedman test: $\chi^2(2)$ =10.75, p=0.0046). Further post-hoc analysis showed that the R^2 value obtained using the unsupervised neural-drive approach was significantly higher than that obtained using either the sEMG-Amp approach (index: $t(7)$=4.64, p= 0.0015; ring-little: p = 0.039) or the sEMG60-Amp method (index: $t(7)$=5.34, p= 0.0016; ring-little: p= 0.016).

Similarly, Fig. 4(b) shows a significant overall difference in RMSE values for the index finger (One-way RM ANOVA: $F(2,14)$ =20.95, $p<0.001$) and the ring-little finger (Friedman test: $\chi^2(2)$ =10.75, p =0.0046). Further post-hoc analysis showed that the RMSE value obtained using the unsupervised neural-drive approach was significantly higher than that obtained using either the sEMG-Amp approach (index: $t(7)$=-3.35, p= 0.0061; ring-little: p= 0.012) or the sEMG60-Amp method (index: $t(7)$=-4.67, p= 0.0022; ring-little: p= 0.012).

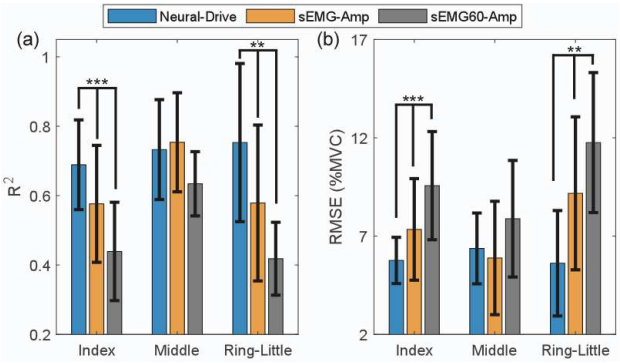

Fig. 4. Comparison of the force prediction performances for each finger. ** denotes 0.001<p<0.01, *** denotes p<0.001.

For the middle finger, no significant differences using the three methods were detected in both R^2 values (Friedman test: $\chi^2(2)$ =4, p=0.14) and RMSE values (One-way RM ANOVA: $F(2,14)$ =1.01, p=0.39). This may be due to a relatively large spatial distance between the forearm activation areas for the middle finger and that of the other two fingers, resulting in minimal crosstalk from the other fingers [8].

IV. Conclusion

In this study, we developed an unsupervised neural-drive approach with consideration of finger muscle co-activations for simultaneous and concurrent multi-finger predictions. MUs extracted from single-finger trials were directly used for the MU extraction of multi-finger tasks. We implemented the MU weight assignment and sharing procedures to better align the force contribution of each MU to corresponding fingers, and then applied these weighted and shared MUs to predict finger forces. Consequently, our method significantly surpassed both supervised sEMG-amplitude approaches, which showed great potential to broaden application scopes, including aiding individuals with hand disabilities. In the future, we will validate our developed model for other types of motor tasks, such as finger flexion movements. Furthermore, we will test the effectiveness of our approach on subjects with hand disabilities, such as arm amputees.

References

[1] H. P. Singh and P. Kumar, "Developments in the human machine interface technologies and their applications: a review," *J. Med. Eng. Technol*., vol. 45, no. 7, pp. 552–573, Oct. 2021.

[2] L. Meng et al., "User-Tailored Hand Gesture Recognition System for Wearable Prosthesis and Armband Based on Surface Electromyogram," *IEEE Trans. Instrum. Meas.*, vol. 71, pp. 1–16, 2022.

[3] L. Zongxing et al., "Human-machine interaction technology for simultaneous gesture recognition and force assessment: A Review," *IEEE Sens. J.*, 2023.

[4] L. Meng et al., "Evaluation of decomposition parameters for high-density surface electromyogram using fast independent component analysis algorithm," *Biomed. Signal Process. Control*, vol. 75, p. 103615, 2022.

[5] R. Roy, Y. Zheng, D. G. Kamper, and X. Hu, "Concurrent and Continuous Prediction of Finger Kinetics and Kinematics via Motoneuron Activities," *IEEE Trans. Biomed. Eng*., vol. 70, no. 6, pp. 1911–1920, 2023.

[6] Y. Zheng and X. Hu, "Concurrent estimation of finger flexion and extension forces using motoneuron discharge information," *IEEE Trans. Biomed. Eng*., vol. 68, no. 5, Art. no. 5, 2021.

[7] D. Farina et al., "Man/machine interface based on the discharge timings of spinal motor neurons after targeted muscle reinnervation," *Nat. Biomed. Eng*., vol. 1, no. 2, Art. no. 2, 2017.

[8] Y. Zheng and X. Hu, "Concurrent prediction of finger forces based on source separation and classification of neuron discharge information," *Int. J. Neural Syst*., vol. 31, no. 06, Art. no. 06, 2021.

[9] N. Rubin, Y. Zheng, H. Huang, and X. Hu, "Finger force estimation using motor unit discharges across forearm postures," *IEEE Trans. Biomed. Eng*., vol. 69, no. 9, pp. 2767–2775, 2022.

[10] A. Hyvärinen and E. Oja, "Independent component analysis: algorithms and applications," *Neural Netw*., vol. 13, no. 4–5, Art. no. 4–5, 2000.

[11] E. A. Clancy and N. Hogan, "Probability density of the surface electromyogram and its relation to amplitude detectors," *IEEE Trans. Biomed. Eng*., vol. 46, no. 6, Art. no. 6, 1999.